

# Gamma Oscillation Maintains Stimulus Structure-Dependent Synchronization in Cat Visual Cortex

Jason M. Samonds<sup>1</sup> and A. B. Bonds<sup>1,2</sup>

Departments of <sup>1</sup>Biomedical and <sup>2</sup>Electrical Engineering, Vanderbilt University, Nashville, Tennessee

Submitted 26 May 2004; accepted in final form 27 July 2004

**Samonds, Jason M. and A. B. Bonds.** Gamma oscillation maintains stimulus structure-dependent synchronization in cat visual cortex. *J Neurophysiol* 93: 223–236, 2005. First published July 28, 2004; doi:10.1152/jn.00548.2004. Visual cortical cells demonstrate both oscillation and synchronization, although the underlying causes and functional significance of these behaviors remain uncertain. We simultaneously recorded single-unit activity with microelectrode arrays in supragranular layers of area 17 of cats paralyzed and anesthetized with propofol and N<sub>2</sub>O. Rate-normalized autocorrelograms of 24 cells reveal bursting (100%) and gamma oscillation (63%). Renewal density analysis, used to explore the source of oscillation, suggests a contribution from extrinsic influences such as feedback. However, a bursting refractory period, presumably membrane-based, could also encourage oscillatory firing. When we investigated the source of synchronization for 60 cell pairs we found only moderate correlation of synchrony with bursts and oscillation. We did, nonetheless, discover a possible functional role for oscillation. In all cases of cross-correlograms that exhibited oscillation, the strength of the synchrony was maintained throughout the stimulation period. When no oscillation was apparent, 75% of the cell pairs showed decay in their synchronization. The synchrony between cells is strongly dependent on similar response onset latencies. We therefore propose that structured input, which yields tight organization of latency, is a more likely candidate for the source of synchronization than oscillation. The reliable synchrony at response onset could be driven by spatial and temporal correlation of the stimulus that is preserved through the earlier stages of the visual system. Oscillation then contributes to maintenance of the synchrony to enhance reliable transmission of the information for higher cognitive processing.

## INTRODUCTION

Sensory perception relies on the classification of sensory information in relation to past experiences. A neurophysiological correlate has been described based on the relationships between neurons' spike trains and the formation of *cell assemblies* (Hayek 1952; Hebb 1949). The spatiotemporal relationships of spike trains provide a robust and flexible system of classification that provides enhancement through associations (Hebb 1949) and depends on contextual changes, as well as short- and long-term response history (Hayek 1952).

Milner (1974) and von der Malsburg (1981) developed this theory to provide a framework for many perceptual phenomena that remain unexplained. Their elaborations are termed *correlation theory* or *temporal binding theory*, where perceptually related features are linked through correlated firing among subpopulations of cells. The original basis of the cell assembly theory was that relationships were formed between cells based

on anatomical connections (Hayek 1952; Hebb 1949). However, acknowledging the dynamic and adaptive nature of the brain, Hayek (1952) proposed that the formation of cell assemblies might not require actual anatomical changes in synaptic connections. It instead could result from short-term enhancement of synaptic effectiveness (a form of plasticity) generated by changes in the temporal structure of spike trains (von der Malsburg 1981). Short-term plasticity with respect to spike train structure has been demonstrated in a variety of conditions (Dobrunz and Stevens 1999; Lisman 1997; Snider et al. 1998; Tsodyks and Markram 1997; Usrey et al. 1998; Varela et al. 1997).

The spike train structure that induces short-term synaptic plasticity has typically been broken down into 2 classes of patterns, bursts and oscillations. Bursts have been operationally defined from an extracellular perspective as 2 or more spikes with intervals  $\leq 8$  ms (Bair et al. 1994; Cattaneo et al. 1981a,b; DeBusk et al. 1997; Mandl 1993). Intracellular studies have typically shown bursts to be intrinsic, resulting from Na<sup>+</sup> currents (Brumberg et al. 2000; Franceschetti et al. 1995) or Ca<sup>2+</sup> currents (Traub and Miles 1991) that lead to nonlinear changes in firing based on changes in the membrane potential (Agmon and Connors 1989; Gray and McCormick 1996; Traub and Miles 1991). Oscillations occur across longer intervals, reflecting periodic firing usually in the gamma range ( $>30$  Hz), depending on the location in the brain and/or the behavioral state or sensory input (Traub et al. 1999). The biophysical basis and perceptual significance of oscillations remains unclear (for review see Traub et al. 1999).

Here we explore the relationships between spike train structure and the orientation-dependent synchronization of cell assemblies from microelectrode array recordings (Samonds et al. 2004) to explore the behavior of cortical oscillation and synchronization. Our results suggest that at least some component of gamma oscillation arises from extrinsic sources such as feedback, although a bursting refractory period is also a likely contributor to the oscillation. The strength of oscillation was only moderately correlated with the strength of synchronization; however, oscillation was associated with maintenance of synchronization. The overall strength of synchronization was more strongly related to synchrony of the onset transients (defined by relative response latencies). We propose that cortical synchrony originates from coherent spatiotemporal stimulus structure, whereas bursts and oscillations maintain and modulate synchrony by preserving its coordination across cell populations.

Address for reprint requests and other correspondence: A. B. Bonds, Department of Electrical Engineering, Vanderbilt University, 255 Featheringill Hall, 400 24th Ave. South, Nashville, TN 37212 (E-mail: ab@vuse.vanderbilt.edu).

The costs of publication of this article were defrayed in part by the payment of page charges. The article must therefore be hereby marked "advertisement" in accordance with 18 U.S.C. Section 1734 solely to indicate this fact.

## METHODS

## Recording

Details of experimental protocol and procedures are described in detail elsewhere (Samonds et al. 2003, 2004). Experimental procedures were performed under the guidelines of the American Physiological Society and Vanderbilt University's Animal Care and Use Committee. Three cats were anesthetized with propofol and N<sub>2</sub>O and paralyzed with pancuronium bromide. Correct refraction was provided by a combination of contact and spectacle lenses, and correspondence of the *areae centrales* was carefully checked with a reversible ophthalmoscope to ensure registry of binocular stimulation. A 5 × 5 multielectrode array (Bionics, Salt Lake City, UT) was pneumatically inserted to a fixed depth of 0.6 mm (exact recording depth varies because of brain curvature). Twenty-two, 25, and 23 single-unit recordings were simultaneously obtained from *area centralis* of area 17 from the 3 cats.

The isolation and signal-to-noise ratio (SNR) of single-unit recordings from the arrays were very good because of the low electrode impedances (about 250 kΩ). The average peak excursion of an action potential was about ±100 μV, ranging from ±50 to 200 μV. Nearly all channels typically had peak noise less than ±40 μV and most were much lower than ±30 μV. The SNR ranged from 1.5 to 20 (in one case as high as 40), in agreement with previous reports on the Bionics multielectrode array capabilities in cat visual cortex (Nordhausen et al. 1996). No data described in the present article were derived from spike separation from multiunit recordings on a single channel. Bionics spike-sorting software, however, was used to remove noise and artifact. During spike-sorting analysis, we were especially careful to consider waveform shrinkage attributed to burst firing (Harris et al. 2000; Snider and Bonds 1998).

## Stimulation

Drifting sinusoid gratings of 2-s duration (10° aperture on a background with an average mean luminance of 73 cd m<sup>-2</sup>) were presented (binocular stimulation) at a distance of 57 cm on a 21-in. Sony Trinitron monitor (Tokyo, Japan). A refresh rate of 120 Hz prevented any artifactual stimulus-locked oscillation or synchronization (Snider 1997). Four subgroups (or assemblies) of 6 cells each were selected from the recordings based on similar orientation preferences within a subgroup. This provided 24 single cells and 60 pairs of cells for quantitative analysis. There are more pairs of cells than single cells because each group of 6 cells produces 15 possible pairs. We tested each of the 4 assemblies across a 30° range around their preferred orientation at 2° increments. Contrast was fixed at 50%, spatial frequency was fixed at 0.5 c/°, and temporal frequency was fixed at 2 or 3 Hz. These parameters were appropriate to drive essentially all cells responsive to the grating orientation. We collected responses from an average of 516 ± 33 presentations of 2-s duration of each stimulus for autocorrelation, renewal density, and cross-correlation analysis. The relatively large number of samples was required for the original quantitative examination of the data set (Samonds et al. 2004) and is not necessarily required for the analysis described in the present article. Because the latency analysis required monitoring each individual response, we found 50 samples to be more manageable while still yielding statistically reliable results.

## Auto- and cross-correlation

We use methods for quantifying "effective connectivity" (Aertsen et al. 1989; Snider et al. 1998) to produce autocorrelograms and cross-correlograms for single cells and pairs of cells, respectively. The joint poststimulus time histogram (JPSTH) is a 2-dimensional histogram of all joint occurrences between pairs of cells at all possible temporal shifts (for 1-ms bins). For autocorrelation we simply replace *y* with *x* for all previous and future descriptions and equations. From

this raw or observed JPSTH, the cross-product matrix of the individual PSTHs is subtracted

$$D_{x,y}(t_1, t_2) = \langle x(t_1)y(t_2) \rangle - \langle x(t_1) \rangle \langle y(t_2) \rangle \quad (1)$$

The cross-product term in the preceding expression represents the joint firing probability, based on the null hypothesis of independence (but including the effects related to changes in average firing rates of each neuron across time). Thus this expression represents the deviation of the actual joint firing probabilities from this null hypothesis. The subtraction of the cross product of the PSTHs is an alternative method to subtracting the traditional "shift predictor," but can provide a more correct result (Aertsen et al. 1989). The quantity  $D_{x,y}(t_1, t_2)$  is the 2-dimensional cross-covariance matrix. The cross-covariance matrix is then normalized for the firing rate using the SD of the predicted PSTH

$$C_{x,y}(t_1, t_2) = \frac{D_{x,y}(t_1, t_2)}{\sqrt{D_{x,x}(t_1, t_1)D_{y,y}(t_2, t_2)}} \quad (2)$$

The normalized cross-correlogram (cross-correlation histogram [CCH]) or autocorrelogram (autocorrelation histogram [ACH]) is then produced by integrating the 2-dimensional matrix  $C_{x,y}(t_1, t_2)$  or  $C_{x,x}(t_1, t_1)$  along the principal diagonal ( $t_1 = t_2$ ).

Features within autocorrelograms were defined by making quantitative measurements of distinct peaks and valleys: 1) the strength of bursting was quantified by the peak at <8 ms (Bair et al. 1994; Cattaneo et al. 1981a,b; DeBusk et al. 1997; Mandl 1993), 2) the strength of the bursting refractory period (or the first oscillation peak) was quantified by the difference between the valley immediately after the burst peak and the next peak (after the bursting peak), and 3) the strength of oscillation was quantified by the difference between the second valley and the second oscillation peak. The strength of synchrony was quantified in a similar manner by measuring the peak in the CCH (at or near a lag time of 0 ms).

We considered alternative methods of measuring gamma oscillation based on Fourier analysis or fitting Gabor functions to the autocorrelogram (König 1994), but both methods are confounded by the dip of the burst refractory period, which leads to false indications of oscillation or an overestimation of the strength of oscillation (Bair et al. 1994; Young et al. 1992). Measurements based on the first oscillation peak alone would also produce the same problem. Therefore cells were classified as oscillatory when the ACH contained a secondary oscillation peak that was at least twice the magnitude of the random fluctuations in the ACH (0.1–0.3%). Subsequent analysis described below shows that the secondary peak is only weakly related to the refractory period and bursting. Reliance on the second peak of the ACH to quantify oscillation thus minimizes the possible confound with the refractory period. In some cases, third and fourth oscillation peaks were present that were also above the noise level in the ACH. The frequency of oscillation in those cells with a second peak in the ACH meeting the criteria described above was quantified by calculating the discrete Fourier transform (0–500 Hz) of the ACH and noting the peak Fourier energy between 20 and 60 Hz.

## Renewal density analysis

Renewal density analysis was used to determine the serial dependency of oscillation (Lebedev and Wise 2000; Mountcastle et al. 1969, 1990). We randomly shuffled the order of the intervals for each response trial and repeated the autocorrelation analysis described above to produce the renewal density histogram (RDH). Any reduction in the oscillation in the RDH signifies serial dependency on the intervals, suggesting an extrinsic source of oscillation (Lebedev and Wise 2000; Mountcastle et al. 1969, 1990). With an external source of oscillation, such as feedforward or feedback, the neuron can still fire spikes within the "quiet interval" of an oscillation. Shuffling the spike intervals will eliminate a portion of the oscillation intervals and in turn

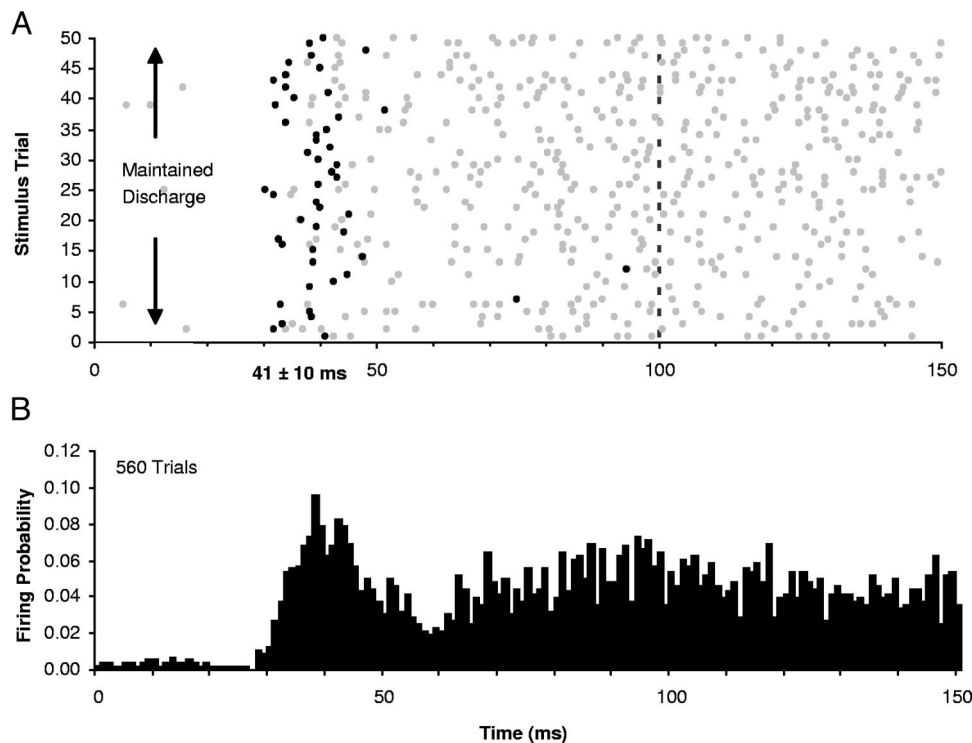


FIG. 1. Response latency or first spike time measurements. *A*: scatter plot of spike times for the first 50 response samples. Black points are the first spike times responding to visual stimulation. *B*: poststimulus time histogram (PSTH) of the same response as *A* using all 560 response samples.

reduce the oscillation in the RDH. An intrinsic source of oscillation, such as membrane hyperpolarization, absolutely prevents the neuron from firing during the “quiet interval” of an oscillation. In this case the oscillation interval is preserved after shuffling the order of the spike intervals and a reduction of oscillation is not seen in the RDH. Although a reduction in the oscillation in the RDH suggests extrinsic involvement, it does not exclude contributions to the oscillation by intrinsic factors.

### Temporal dynamics of the CCH

Two-dimensional CCHs were produced using sliding-window analysis (Castelo-Branco et al. 1998; Gray et al. 1992; Nase et al. 2003; Neuenschwander et al. 2002). Although simply examining  $C_{x,y}(t_1, t_2)$  before integrating across the diagonal would reveal the temporal dynamics of the synchrony at a 1-ms resolution, too much noise is present in the matrix for meaningful interpretation of the temporal dynamics of synchrony. Sliding-window cross-correlation analysis simply reflects sliding-window averaging of  $C_{x,y}(t_1, t_2)$  to reduce the noise. We use a window of 200 ms width at a bin resolution of 50 ms.

### Measuring latency

When looking at individual or averaged PST histograms across time, within the first 100 ms cortical cells have a transient peak with a relatively high probability of firing or average firing rate (Ghose and Freeman 1992). In some cases, we found that the transient probability of firing could be as high as 0.8 for 5-ms bins (or an average firing rate 160 sps). The initial peak is followed by a relaxation, after which there can be a secondary peak representing the sustained response of both simple and complex cells. Simple cells have additional peaks in the firing rate caused by the temporal frequency of the drifting sinusoid grating.

To determine latency, we measured the first-spike time within a 100-ms window for single cells (see Fig. 1*A*) and the difference between first-spike times within a 100-ms window between pairs of cells. Data were included only for cells with responses within the

window in  $\geq 75\%$  of the trials. We measured first-spike times on only the first 50 data samples for each cell and pair of cells because direct observation of the individual responses was necessary to ensure that maintained activity (see Fig. 1*A*) was not mistaken for first spikes in response to visual stimulation. Maintained activity was usually apparent only in complex cells. In these cells the transient peak was generally strong, making the first spike (as a response to the stimulus and not maintained activity) easily identifiable. The difference between the average latency determined from the transient peak in the PSTH (using all  $516 \pm 33$  samples) and determined from the first-spike time procedure described above (using the first 50 samples) was not statistically significant (*t*-test,  $P > 0.4$ ).

In some cases, the secondary peak in the PSTH was much larger than the transient peak (e.g., see Fig. 2). For these cells, we applied the spike time measurements and 75% criterion to a 200-ms window around the secondary peak (using the same procedure described above). A larger window was chosen because the secondary peak is typically broader than the transient peak. The difference between the average latency measured from the secondary PSTH peak (using all  $516 \pm 33$  samples) and measured from spike times from 50 samples was again not statistically significant (*t*-test,  $P > 0.49$ ). We also tested the reliability of the response latency differences on a trial-by-trial basis by measuring the SD across the 50 trials.

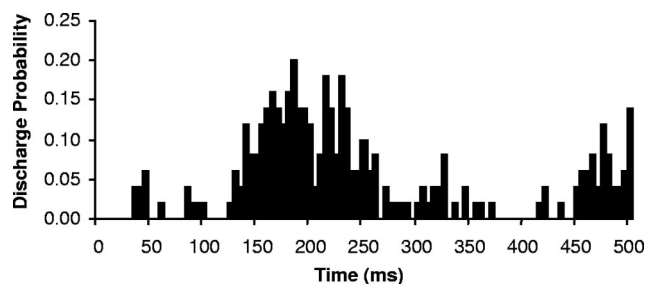


FIG. 2. Example PSTH of a response with a relatively weak transient peak and a much more prevalent secondary peak.

## RESULTS

We examined 24 single cells and 60 pairs of cells from four 6-cell assemblies (each 6-cell group contains 15 possible pairs) recorded with a Bionics  $5 \times 5$  microelectrode array in area 17 of 3 anesthetized and paralyzed cats (Samonds et al. 2004). We first analyzed the single-cell spike trains using autocorrelation and renewal density analysis (see METHODS) to quantify the bursting, oscillation, and serial dependency of interval information. We examined the possible underlying mechanisms of the oscillation and bursting refractory period found in the ACH. After quantifying the temporal structure of the spike trains, we inspected the relationship between the structure and the cross-correlation between pairs of cells (i.e., synchrony). We also inspected the temporal dynamics of the synchrony. Finally, after comparing orientation-dependent changes of the structure and synchrony, we tested how latency differences (i.e., synchronization of the input) and orientation-dependent changes in latency were related to the overall strength of cortical synchronization.

*Autocorrelation and renewal density analysis*

Figure 3, A, B, and C represent the 3 basic qualitative *autocorrelation histogram* (ACH) patterns (black lines) we find for the 24 cells we examined. The ACH has been normalized for the firing rate, as well as for temporal modulations in the firing rate (Aertsen et al. 1989; see METHODS for details). The same procedure was previously used to produce *cross-correlation histograms* (CCH) (Samonds et al. 2003; Snider et al. 1998). The ACH is plotted as the percentage of the maximum possible ACH value (i.e., if all spikes were correlated) with the aforementioned normalization procedure.

All 24 cells showed a noticeable peak in the ACH at 2–5 ms (see Fig. 3, A, B, and C) signaling the predominance of bursting intervals in the responses. The peak of the burst intervals averaged  $2.9 \pm 1.1$  ms (mean  $\pm$  SD). This peak reaches a clear minimum around 8 ms, providing an operational criterion for

classification of burst spikes (Bair et al. 1994; Cattaneo et al. 1981a,b; DeBusk et al. 1997; Mandl 1993). In 5 out of 24 cells, the ACH showed little or no modulation beyond the bursting peak (e.g., Fig. 3A). The ACH was either relatively flat or had a slight decay. Note also that the 1-ms autocorrelation value (the value is actually below zero in all cases; not shown) represents the refractory period of the spiking mechanism of the cell, which limits its maximum firing rate.

The remaining 19 out of 24 ACHs showed a clear valley immediately after the bursting peak (Fig. 3, B and C), which corresponds to the *bursting refractory period* centered at about 8 ms found in interspike interval (ISI) histograms (Bair et al. 1994; DeBusk et al. 1997; Snider et al. 1998; Young et al. 1992). The term “refractory period” in this case is used to describe an absence of intervals over an intermediate range reflecting the short “silent” period following a burst. The average center of the refractory period was  $10.5 \pm 2.7$  ms, ranging from 8 to 17 ms. Fifteen out of the 24 ACHs (or 63% of the 24 single cells) also had a clear secondary peak (Fig. 3C) signifying oscillatory firing, which fell within the gamma range (30–60 Hz).

We determined the frequency of the oscillation by measuring the peak between 20 and 60 Hz of the Fourier transform of the ACH (Fig. 3D). The secondary peak in Fig. 3C leads to a clear peak at 43 Hz in Fig. 3D. The average frequency for the 15 cells that exhibited gamma oscillation was  $49.8 \pm 4.5$  Hz (range 43–54 Hz). The SD of the frequency of oscillation is significantly smaller (mean = 2.2 Hz) when we examine each 6-cell assembly independently (*F*-test,  $P < 0.06$ ).

We also wanted to determine whether the oscillation we found in the ACH was an intrinsic property of the cell membrane (e.g., Gray and McCormick 1996; Nowak et al. 2003) or an extrinsic property resulting from, say, GABAergic interneuronal networks (Cunningham et al. 2003; Traub et al. 1999, 2003). We compared the *renewal density histogram* (RDH; gray line in Fig. 3C) to the ACH (the original autocorrelation histogram described above; black lines) to assess the influence

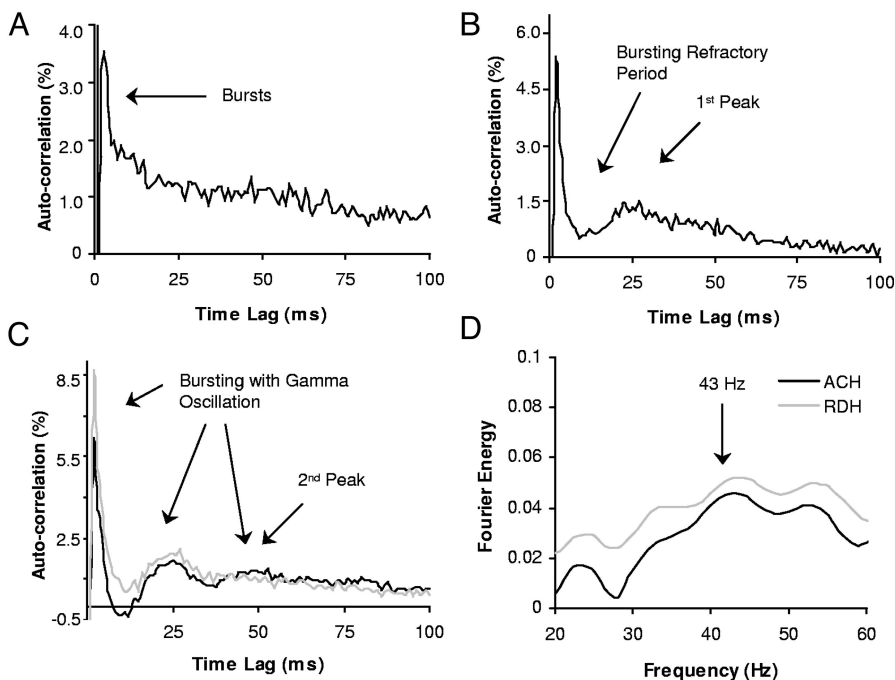


FIG. 3. Examples of autocorrelation properties. A: response with bursting. B: response with bursting and bursting refractory period (autocorrelation histogram [autocorrelation histogram, ACH] and interval-shuffled ACH or renewal density histogram [RDH]). C: response with bursting and gamma oscillation. D: Fourier transform of C, oscillation frequency = 43 Hz. Note: autocorrelation values correspond to normalized measurements described in METHODS.

of extrinsic factors on oscillation. If the oscillation in a spike train is extrinsically driven, the ACH will depend on the serial order of the ISIs (Lebedev and Wise 2000; Mountcastle et al. 1969, 1990; see METHODS for details). The RDH is calculated in the same manner as the ACH described above except the intervals for each response are randomly shuffled. A reduction in the periodicity of the ACH after random shuffling of the ISIs (i.e., the RDH) reflects contributions from external influences (Lebedev and Wise 2000; Mountcastle et al. 1969, 1990). This is because intrinsic (membrane-based) oscillation, such as hyperpolarization, will likely result in absolute silence between spike clusters, whereas with an external source of oscillation, spikes can still occur between the oscillation intervals. A reduction of periodicity in the RDH does not, however, rule out additional contributions from intrinsic properties.

We found no reduction in the RDH in only 3 out of 19 cells (of these 3 cases, 2 had gamma oscillation). In the other 16 RDHs, the periodicity was clearly reduced with both a decrease in the depth of the refractory period valley and decreases in the 2 oscillatory peaks. Overall, the ACHs tended to “flatten” out. Figure 1C shows an example of the reduction (gray lines) in the periodicity of the RDH. The reduction is also clear in the Fourier analysis with the 43-Hz peaks becoming less prominent (Fig. 3D).

The reduction in the RDH does not appear to arise simply because the responses contain both short-interval (<8 ms) and long-interval (>15 ms) structures. All 3 cells that showed no reduction in the RDH also demonstrated both bursts (short-interval structure) and a bursting refractory period (long-interval structure). Additionally, 2 of these cells exhibited gamma oscillation. We therefore believe that the reduction in the RDH observed in the other 16 cells represents influences beyond what might be expected from the combined presence of short- and long-interval structures and suggests some tangible external influence on the gamma oscillation. However, those 2 cells showing gamma oscillation but no RDH reduction demonstrate that intrinsic properties of the cells can also play a considerable role in producing the gamma oscillation.

To quantify the serial dependency of oscillation across our population of cells, we quantified the strength of the oscillation in the ACH by: 1) the first oscillation peak (difference between the burst refractory period valley and the first oscillation peak) and 2) the second oscillation peak (the difference between the second valley and the second oscillation peak). Figure 4 shows the average values we measure for the 2 oscillation peaks observed in the ACH (black) and the shuffled RDH (gray). The first and second oscillation peaks are reduced by 31 and 34%, respectively, from the ACH to the RDH, presumably reflecting significant contributions to the oscillation from extrinsic factors (*t*-test,  $P < 0.02$  and  $P < 0.007$ , respectively).

#### Bursting refractory period

The bursting refractory period can suggest the presence of a first oscillation peak in the ACH even though it may be absent, thus leading to a mistaken identification of gamma oscillation (Bair et al. 1994; Young et al. 1992). Conversely, measurements of the bursting refractory period can be confounded by the oscillation. For example, our measurement of the first oscillation peak in the ACH and RDH (above) might suggest the bursting refractory period is produced by extrinsic factors.

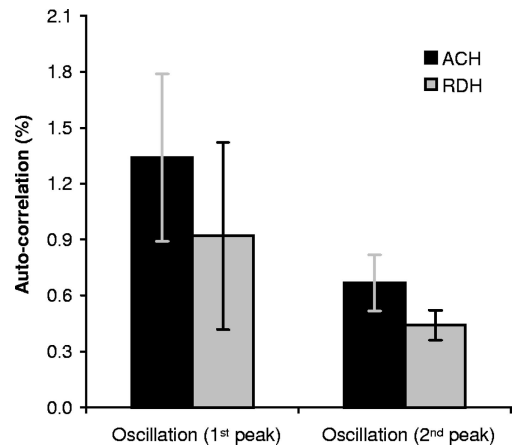


FIG. 4. Average ACH and RDH measurements (with SE bars for  $n = 15$  single cells) for the first and second gamma oscillation peaks.

However, most intracellular studies clearly find an intrinsic afterhyperpolarization (AHP) after bursts that would produce the refractory period (Agmon and Connors 1989; Brumberg et al. 2000; Connors and Gutnick 1990; Franceschetti et al. 1995; Gray and McCormick 1996; Nowak et al. 2003; Silva-Barrat et al. 1992; Traub and Miles 1991).

If the bursting refractory period results from an AHP after a burst, the probability of firing within this refractory period nears zero. The cell does not necessarily *have* to fire a spike immediately after the AHP. There will be more instances of ISIs corresponding to the AHP (and the bursting refractory period) when the cell *does* fire immediately after the AHP, which would be more likely with higher average firing rates. Therefore if the bursting refractory period reflects an intrinsic property such as an AHP, there should be correlation between the strength of the bursting refractory period and the firing rate (and the highest possible firing rate would in effect be limited by this AHP and refractory period). Figure 5A demonstrates there is a relatively strong relationship between the refractory period measurement and the firing rate ( $R^2 = 0.48$ ), suggesting that an AHP is the source of the refractory period.

We also wanted to find out whether chattering cells reported in layers 2/3 of the visual cortex contributed to the gamma oscillation in our recordings. Chattering is formed by bursts of 2–5 spikes that oscillate in the gamma range and the firing pattern is believed to be intrinsic, resulting from suprathreshold stimulation (Gray and McCormick 1996; Nowak et al. 2003). The results reported above suggest that oscillation appears to have at least some component of extrinsic input. By examining the relationship between bursts and oscillation, we hoped to determine the extent to which oscillation arises from a burst AHP (intrinsic) or from more coordinated feedback (extrinsic). In addition, we also examine the relationship between the refractory period and bursts to increase assurance that the refractory period does indeed arise from bursts.

Figure 5B presents a scatter plot of the refractory period and oscillation measures against bursting. The correlation between bursts and the refractory period is moderate ( $R^2 = 0.27$ ), whereas there is almost no correlation between the bursts and oscillation ( $R^2 = 0.06$ ). We thus propose that there is a refractory period likely resulting from an AHP (Fig. 5A) that is a property of bursts (Fig. 5B). However, we do not see a strong

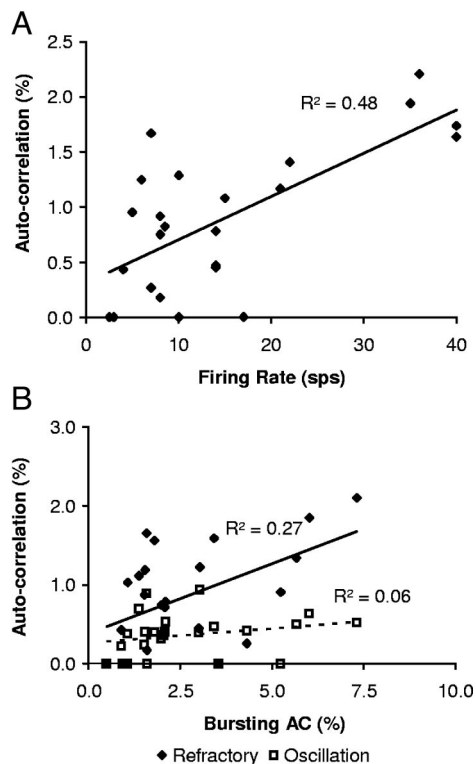


FIG. 5. Scatter plots and regression analysis ( $n = 24$  single cells) to examine the properties of the refractory period. *A*: bursting refractory period vs. the average firing rate for each cell. *B*: bursting refractory period and oscillation vs. bursts.

link between oscillation and the presumably intrinsic bursting and AHP (Fig. 5*B*).

We emphasize that the extracellular recordings from our sample of cells do not reveal the underlying biophysical processes that generate temporal structure in single-cell cortical responses. We are merely attempting to quantify the bursting, bursting refractory period, and gamma oscillations in the context of the net output of the cell so that we can test their statistical relationships with the synchronization between groups of cells. Our analysis of extrinsic versus intrinsic sources is simply to provide some reference between our data and the intracellular results reported on these phenomena.

#### Temporal structure and synchronization

Eckhorn et al. (1988) and Gray et al. (1989) proposed that gamma oscillations drive synchronization across larger cortical distances ( $>2$  mm) when the cells share similar orientation preferences and are coherently stimulated with a single bar of light. The phase locking of the oscillatory activity was present for shorter distances as well. The dimensions of our microelectrode array ( $5 \times 5$ ) yielded cell pairs as close as  $400 \mu\text{m}$  (electrode spacing) and as far as 2 mm, with both overlapping and nonoverlapping receptive fields (Samonds et al. 2004). In this section, we examine the relationship between the temporal structure (with an emphasis on the gamma oscillation) and synchronization. We again use the normalized JPSTH analysis to produce a CCH. Again, correlation is quantified as the percentage of the maximum possible correlation.

Figure 6 is an example of 3 cells that are synchronized when driven by the same orientation. We show only 2 of the CCHs

to provide examples of 2 cases of very strong synchronization that have different characteristics. Figure 6*D* is the CCH between one cell with very weak temporal structure (Fig. 6*A*; cell 8) and another cell with very strong gamma oscillation (Fig. 6*B*; cell 13). In spite of the lack of oscillation in one of the 2 cells, there is still very strong synchronization with a lag time of 0 ms, but no oscillation is apparent in the CCH (Fig. 6*D*). For these 2 cells, the receptive fields were partially overlapping (data not shown), suggesting some common input. In our second example, both cells (Fig. 6, *B* and *C*; cells 13 and 11, respectively) have strong gamma oscillation, which is then reflected in their CCH (also 0-ms lag time; Fig. 6*E*). The receptive fields of these 2 cells were also partially overlapping.

We compared the influence of our 3 ACH measurements (see Fig. 3 and METHODS for details) on synchrony by plotting the normalized CCH peak (near 0 ms) versus the average value (between the 2 cells) of both of the normalized autocorrelation quantities for bursts and oscillation (Fig. 7). Both forms of temporal structure were only moderately correlated to the amount of synchrony between the 2 cells. The bursts had a slightly weaker relationship ( $R^2 = 0.17$ ) than oscillation ( $R^2 = 0.22$ ).

To probe deeper into the relationship between oscillation and synchrony, we examined the temporal dynamics of correlation. Figure 8, *A* and *B* display the temporal dynamics for the 2 CCHs of Fig. 6, *D* and *E*, respectively. The synchrony in Fig. 8*B* (between 2 oscillators) maintains its strength over time, whereas the synchrony in Fig. 8*A* (CCH has very little oscillation) decays over the stimulus duration. The peak correlation decreases by 25% after 2 s of stimulation and the decay is even more obvious when observing the strength of the correlation over a wider window of lag times.

Similar results are found when looking at all 60 pairs of cells analyzed for synchronization. We measured an average peak cross-correlation of  $1.2 \pm 1.0\%$  for 52 out of 60 pairs of cells (range: 0.2–3.9%) that had a peak magnitude that was at least twice the magnitude of the random fluctuations in the CCH. However, only 39 out of 60 pairs had CCH values that were at least double the random fluctuations when examining the temporal dynamics of the synchrony. Twenty out of 39 pairs did not have a secondary oscillation peak that met our criteria (see METHODS) in one or both ACHs and in the CCH. Fifteen out of these 20 pairs had a decay of relative synchrony during the stimulus period. During 2 s of visual stimulation the synchrony decayed on average from 1.4 to 0.7% (Fig. 9, *right*; *t*-test,  $P < 0.03$ ). The data were insufficiently consistent (or the stimulation time was not long enough) to perform more rigorous characterization of the decay time constants (using peak measurements or integrating across a window of lag times). All 19 pairs of cells *with* gamma oscillation in both ACHs and the CCH maintained their relative synchrony throughout visual stimulation. During 2 s of visual stimulation the synchrony was reduced on average from 2.1 to 2.0% (Fig. 9, *left*; the slight decrease is not statistically significant: *t*-test,  $P > 0.34$ ).

Previously, Ts'o et al. (1986) proposed that horizontal connections between orientation columns would lead to the orientation-dependent synchrony across longer distances. However, the phase difference of the synchronization is generally 0 ms, making it unlikely that synchronization relies on direct serial synaptic connections between the analyzed cell pairs, although the absence of a shift in the CCH is not an unambiguous

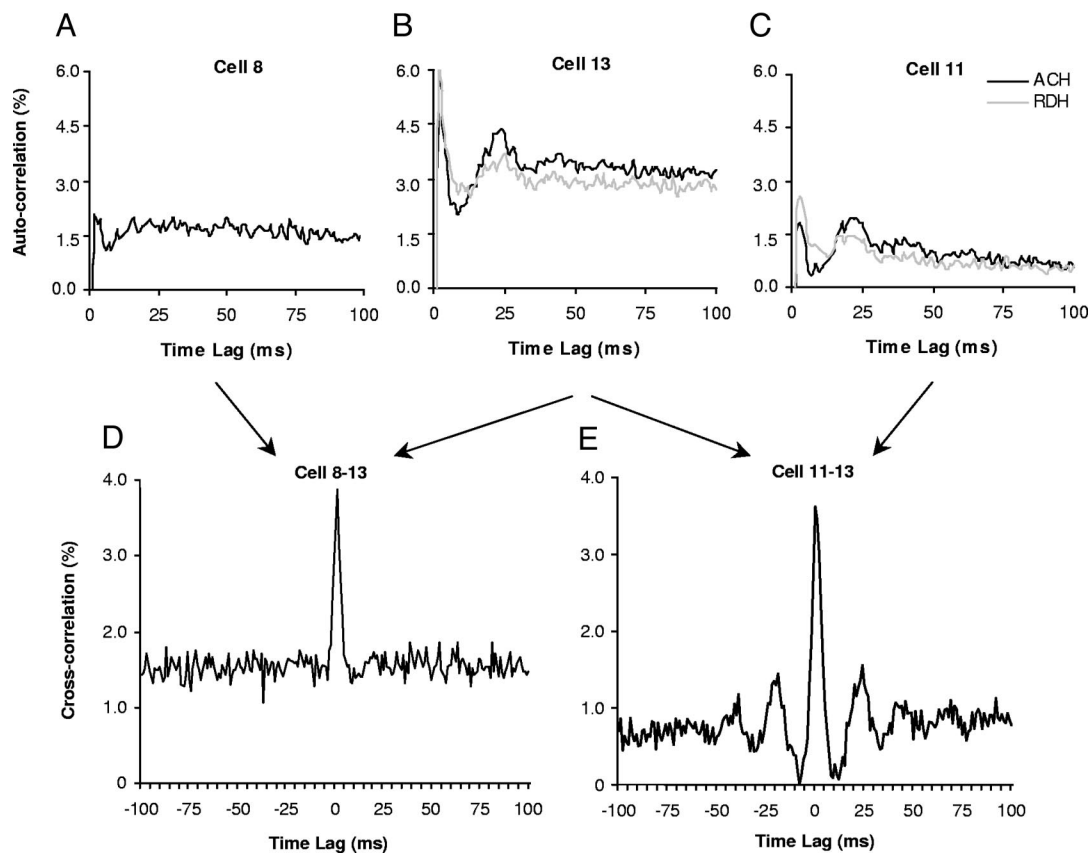


FIG. 6. Strong synchrony occurs with and without oscillation. *A*: autocorrelation without oscillation. *B* and *C*: autocorrelations with oscillation. *D*: synchrony (not showing oscillation) between a nonoscillator (*A*) and an oscillator (*B*). *E*: synchrony (showing strong oscillation) between 2 oscillators.

indicator of synaptic pathways (Aertsen et al. 1989). Forty out of the 52 peaks in the CCHs were centered at 0 ms, implying no role for synaptic delay, and only 8 out of the 52 peaks differed by more than 2 ms (ranging from 3 to 4 ms), with an average lag time of the CCH peak of  $0.8 \pm 1.2$  ms.

*Orientation-dependent changes in structure*

Varying the orientation of a visual stimulus leads to changes in the number of spikes in a burst (burst length). For a constant firing rate, nonoptimal orientations reduce burst length (DeBusk et al. 1997). This variation in burst length can also be

viewed as bursts being tuned for orientation with greater selectivity than that of the total spike count (Cattaneo et al. 1981a). Because longer bursts yield a higher probability of postsynaptic spiking (Snider et al. 1998), correlation is also more selective for orientation than the firing rate. Oscillation has been found to be tuned for orientation as well (Friedman-Hill et al. 2000; Frien and Eckhorn 2000; Frien et al. 2000).

Figure 10 is an example of the tuning of temporal structure for orientation. At first glance, the ACH features (Fig. 10, *A* and *B*) and CCH peaks (Fig. 10*C*) do not appear to be highly selective for orientation. However, we are examining only a  $30^\circ$  range of orientation and both the ACH and CCH are normalized for changes in the firing rate. Therefore *any* observed change with respect to orientation means that the feature is more selective for orientation than is the firing rate. Previous analysis on these data found the synchrony to have a half-height bandwidth on average 31% narrower than the average firing rate (Samonds et al. 2004). Figure 10 thus presents a representative example confirming that bursts, oscillation, and correlation are all more spatially selective than the average firing rate (Cattaneo et al. 1981a; DeBusk et al. 1997; Frien and Eckhorn 2000; Frien et al. 2000; Samonds and Bonds 2004; Samonds et al. 2003, 2004; Snider et al. 1998).

Gamma oscillation is typically obvious in multiunit and local field potential analysis (Eckhorn et al. 1988; Friedman-Hill et al. 2000), although it has been much more elusive in isolated single-unit studies (Bair et al. 1994; Bringuier et al. 1997; de Oliveira et al. 1997; Molotchnikoff et al. 1996; Nowak et al. 1999; Tovee and Rolls 1992; Young et al. 1992).

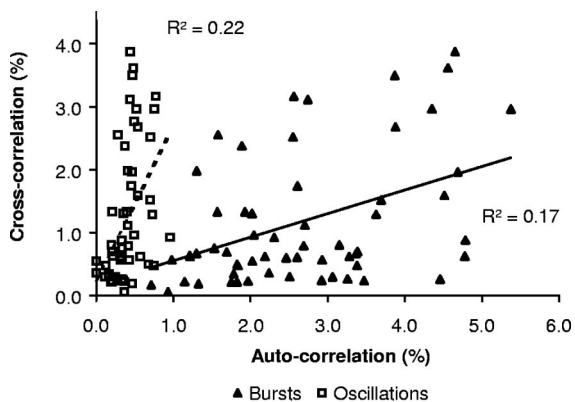


FIG. 7. Scatter plots and regression analysis ( $n = 60$  pairs of cells) for the relationships between average pairwise ACH properties and cross-correlation histogram (CCH) properties.

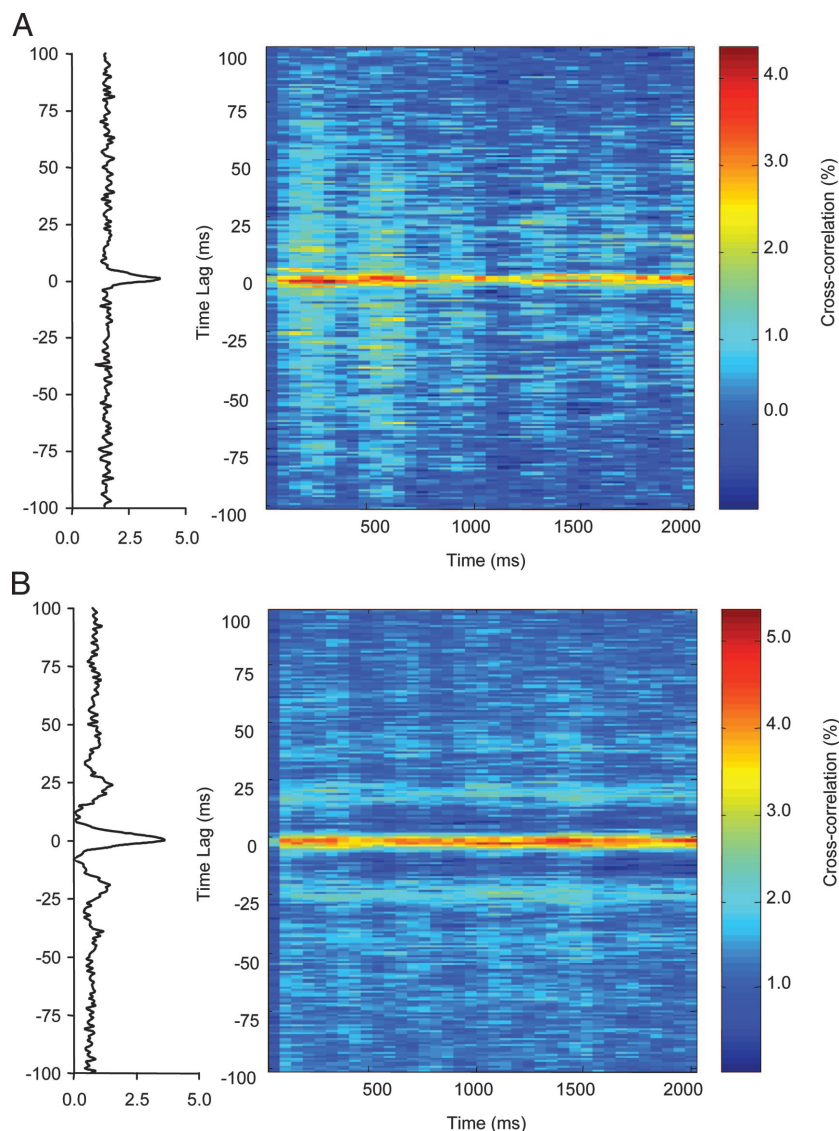


FIG. 8. Sliding-window (200 ms) temporal dynamics (50-ms resolution) of the CCH in *A*, Fig. 5*D* (nonoscillatory decay in synchrony) and *B*, Fig. 5*E* (sustained synchrony with oscillation).

In our experience, oscillation can be very difficult to detect in single units because it can be very selective for orientation. For example, in the cell of Fig. 10*A*, oscillation only occurred over a 6° range of orientation and was relatively weak. Testing of

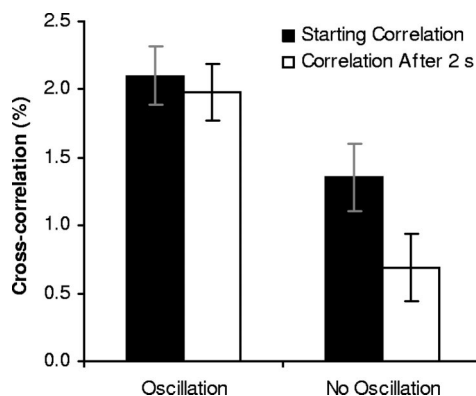


FIG. 9. Average initial and end of stimulation (2 s) CCH peak measurements for oscillatory ( $n = 19$ ) and nonoscillatory ( $n = 20$ ) synchronization (error bars are SE).

orientation at 2° increments thus increased our chances of observing small amounts of gamma oscillation in single units.

Figure 10 also shows that the correlation (synchrony) appears to be more selective to orientation than bursts. Snider et al. (1998) found that the correlation varied even beyond what changes in the burst length would predict and proposed that coincident inputs might also play a role in the synaptic efficacy (see also Samonds and Bonds 2004; Samonds et al. 2003). The narrow selectivity of oscillation (Fig. 10*A*) is an alternative explanation of the narrow selectivity of correlation, but the relatively moderate relationship between oscillation and synchrony (Fig. 9) suggests that other factors influence orientation-dependent changes in synchronization. In the next section, we explore how stimulus-induced timing relationships between responses among an assembly of cells are related to cortical synchronization.

*Coincidence detection and orientation-dependent phase shifts*

In a previous study (Samonds and Bonds 2004), we showed that orientation information is contained in the spike timing (in the form of temporal shifts in the response) and proposed that

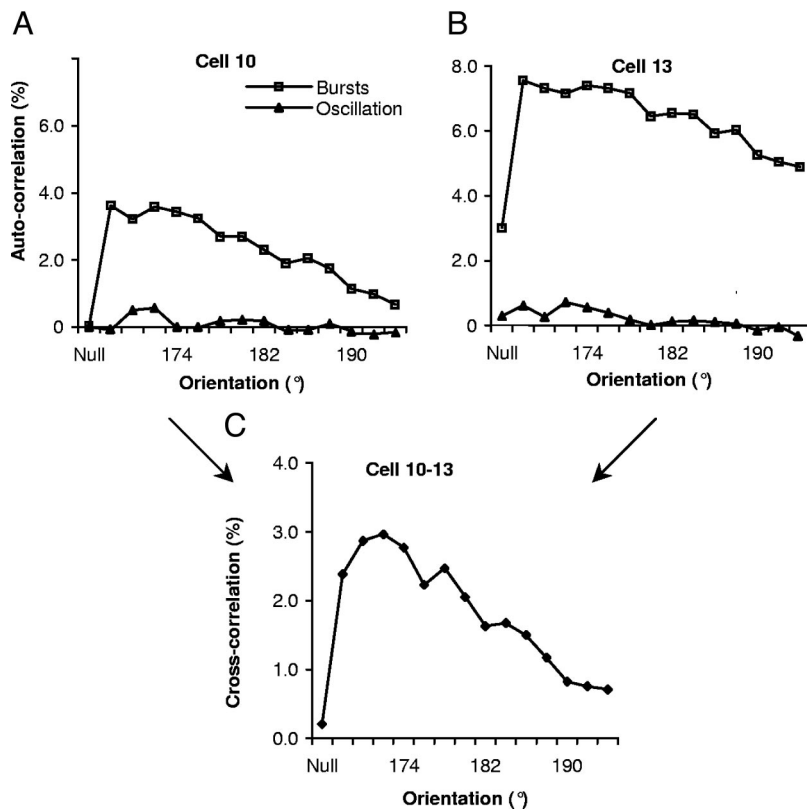


FIG. 10. Stimulus dependency of bursts, oscillation, and synchronization. *A*: example of variation of bursts and oscillation with respect to the orientation of the grating (quantities normalized for firing rates). *B*: another example of orientation dependency of the temporal structure (notice the small orientation range of oscillation for both *A* and *B*). *C*: orientation dependency of the synchrony between the cells in *A* and *B*.

it resulted simply from the relationship between a visual stimulus and the spatiotemporal properties of the receptive field (particularly off-centered relationships; see Fig. 11, *A* and *B*). Because response latency is correlated between cells across trials (Fries et al. 2001), we speculated that stimulus-dependent relative time shifts would be reflected in the synchrony among cell assemblies and could be decoded by means of coincident detection. Figure 11, *C–F* (*left vs. right*) provides a clear example of an orientation-dependent timing shift in the response. When a  $174^\circ$  drifting grating is presented, the response latencies for the 2 cells are the same (Fig. 11*C*, white arrow). When the grating is rotated by  $10^\circ$  (to  $184^\circ$ ), the response latencies now differ, with the response for cell 10 (gray) arriving about 50 ms later (Fig. 11*D*, black arrow). Figure 11, *E* and *F* confirm the relationship between latency and synchrony (Fig. 11, *A* and *B*) by showing that the synchrony is nearly halved when the latencies are out of phase. The example in Fig. 11, *C–F* represents simple cell responses, with very strong modulation that is coupled to the drift rate. However, information on orientation resulting from response latency shifts is also seen in complex cell responses, with little or no rate modulation (Samonds and Bonds 2004).

To summarize this result across all of our data, we measured both the latency and the relative latency (i.e., latency difference) between pairs of cells. We include only the data where  $\geq 75\%$  of the trials had a spike within a 100-ms window. Because responses characteristically have a strong onset transient peak in the PST ( $< 100$  ms) followed by another strong, but broader, peak (about 200–300 ms) at the start of the sustained response, we sometimes used the secondary peak (using a 200-ms window) if it was more reliable (i.e., meeting our 75% criteria).

For relative latency, spikes from *both* cells had to be within the 100- or 200-ms window for  $\geq 75\%$  of the trials.

The average transient response latency ( $n = 12$  cells) was  $53.5 \pm 18.2$  ms and the average sustained response latency ( $n = 18$  cells) was  $239.0 \pm 88.1$  ms. The average SD of either the transient or sustained latency ( $n = 18$  cells; from  $n = 50$  stimulus trials) was  $29.5 \pm 16.8$  ms. The average difference between latencies ( $n = 31$  cell pairs) was  $42.3 \pm 42.2$  ms with an average SD ( $n = 31$  cell pairs; from  $n = 50$  stimulus trials) of  $48.5 \pm 24.4$  ms. The difference in latency ranges from 0 to 120 ms, whereas the SD ranges from 11 to 91 ms.

Figure 12 has scatter plots showing the relationship between synchronization and either the difference between latency ( $\Delta$  latency; Fig. 12*A*) or the SD of the difference between latency (SD  $\Delta$  latency; Fig. 12*B*). Both the difference in latency ( $R^2 = 0.50$ ) and the SD of the difference ( $R^2 = 0.53$ ) show strong inversely logarithmic correlation with the cross-correlation peak. This demonstrates that the chance of 2 cells synchronizing is much greater when their response latencies are nearly the same (and reliably so across stimulus trials). Because the synchronization is present from the first moments of the response, we conclude that it is induced by the simultaneity of the input signals and is not developed post hoc throughout the response.

Our criterion for latency analysis requiring responses in  $\geq 75\%$  of the trials biases our analysis to those pairs of cells that have stronger responses, where the response latency is likely to be more reliable. Figure 12*B* might be thus interpreted as simply demonstrating that the strength of synchrony depends on the strength of the response. However, we find almost no correlation between the strength of the synchrony and the average firing rate (Fig. 13).

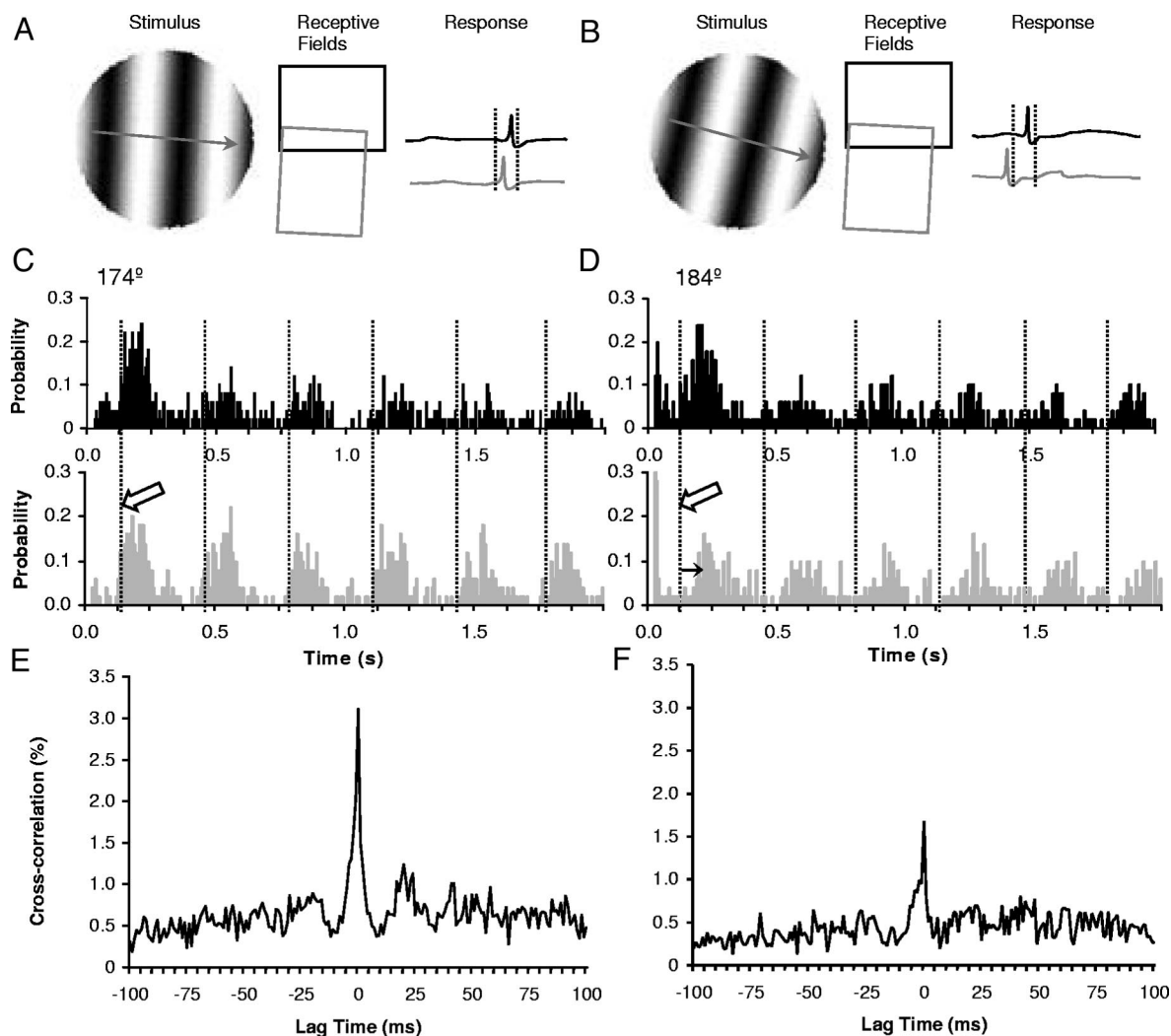


FIG. 11. Relationship between the relative orientation-dependent response latency between cells and synchronization. *B*: PSTHs of activity to  $174^\circ$  drifting grating for 2 simultaneously recorded cells ( $n = 50$  stimulus trials). *C*: PSTHs of activity with a  $10^\circ$  rotation of the grating for the same cells (notice the response for cell 10 is about 50 ms later; black arrow). *D*: CCH for  $174^\circ$  orientated stimulus. *E*: CCH for  $184^\circ$  orientated stimulus.

## DISCUSSION

The primary goal of this study was to determine the underlying mechanisms of the short-term plasticity that can produce cooperative information about orientation (Samonds et al. 2004). When driven by a drifting grating of a particular orientation, distinct groups of cells are strongly synchronized, increasing the chances that their aggregate signal integrates at later stages of visual processing. Even small changes in orientation reduce the synchronization, yielding in effect an *assembly filter* (Samonds et al. 2004). By controlling the effective integration at later stages of visual processing through synchronization, the cortical network limits or filters what collective information is processed. Beyond the creation of this cooperative information, the assembly filter also provides a dynamic mechanism to filter for structure across the visual field because cell assemblies contain both overlapping and nonoverlapping receptive fields. We considered 3 possible sources, each known to be orientation dependent, for this synchronization: 1) gamma oscillations (Eckhorn et al. 1988; Gray et al. 1989), 2) bursting (Snider et al. 1998), and 3) stimulus-dependent timing (Samonds and Bonds 2004).

Before we could measure the statistical relationships between these properties and synchrony, we needed to quantify their respective strengths. Our approach was to analyze properties (bursting, burst refractory period, oscillation) of the autocorrelation analysis (Aertsen et al. 1989) that were suggested by intracellular studies. We then measured the correlation between each property and the synchrony. We found only a moderate relationship between bursts or oscillation and synchronization, suggesting that they are only peripherally associated with synchrony. We found a stronger inverse logarithmic relationship between the cell pairs' response latency differences (as well as the reliability of those differences) with synchrony. This result suggests that those cell pairs that are synchronized must be synchronized for their *first* spikes and that synchrony is not gradually acquired. Interestingly, we do find a possible functional role for oscillation. In most CCHs that do not exhibit any oscillation, synchrony decays over intervals on the order of seconds. All of those CCHs that exhibit oscillation maintain their synchrony, suggesting that oscillation provides a "framework" that prevents the decay.

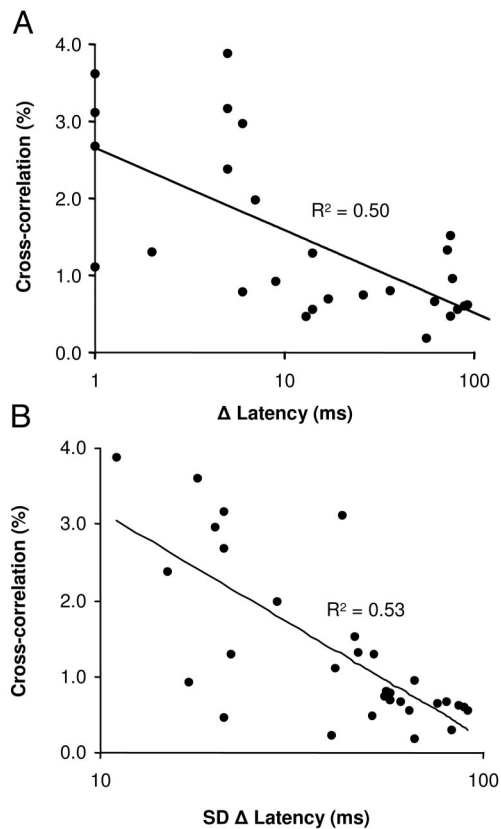


FIG. 12. Scatter plot and logarithmic regression analysis ( $n = 31$  pairs of cells) for the relationship between the synchrony and relative latencies between cell pairs. *A*: cross-correlogram peak vs. the difference between the 2 cells' response latencies. *B*: cross-correlogram peak vs. the SD of the difference between the 2 cells' response latencies.

#### Suprathreshold activation?

Eckhorn et al. (1988) and Gray et al. (1989) demonstrated that cortical cells with similar orientation preferences would synchronize when activated by a single stimulus that spanned across both receptive fields. They proposed that the synchronization supported the temporal binding theory, in which single cells representing individual object features synchronize when those cells are perceptually related (e.g., respond to part of the same object). They also suggested that intracortical oscillation provided a substrate for synchronization of cells across longer cortical distances. Theoretical models have supported the synchronization of oscillators (Ernst et al. 1995, 1998; Grossberg 1976, 1980; Rietboeck et al. 1987; Tsodyks et al. 1993; von der Malsburg and Schneider 1986).

Our results, however, suggest instead that synchrony is a transient phenomenon that occurs for particular groups of cells when they are coherently activated by stimulus structure. Although our results do not prove whether oscillation maintains synchrony or synchrony maintains oscillation, we suggest the transient nature of the synchrony implies the former. Synchronous inputs could trigger the oscillation by suprathreshold potentials but whether oscillation is sustained by feedback circuitry (Cunningham et al. 2003; Traub et al. 2003) or intrinsic sources (Gray and McCormick 1996) also remains unclear. Stimulus-dependent gamma oscillation is found in the membrane potential of hyperpolarized cells (Jagadeesh et al. 1992), but because hyperpolarization of one cell does not

disable the network, that does not rule out a role for feedback in the oscillation. Bursting also requires a suprathreshold potential (Agmon and Connors 1989; Brumberg et al. 2000; Connors and Gutnick 1990; Franceschetti et al. 1995; Gray and McCormick 1996; Nowak et al. 2003; Silva-Barrat et al. 1992; Traub and Miles 1991), suggesting that synchronous inputs encourage both bursts and oscillation. Bursts and GABAergic networks might even be viewed as coincident detectors (Galarreta and Hestrin 2001; Harris et al. 2001). This implies that bursts and oscillation do not actually directly amplify the stimulus information and produce synchrony, but in essence reflect and preserve the salient information from the synchronous inputs by making the relatively weak cortical synaptic connections more effective.

Cortical gamma oscillation has also been suggested as arising from afferent LGN input (Ghose and Freeman 1992, 1997). However, there appear to be 2 forms of oscillation: 1) 60- to 120-Hz oscillation that originates in the retina and is passed on to the LGN and cortex and 2) 30- to 60-Hz oscillation that originates in the cortex and propagates back to the LGN (Castelo-Branco et al. 1998; Neuenschwander et al. 2002). The 60- to 120-Hz feedforward oscillation was transient and decayed (along the same time frame as our nonoscillatory synchrony), whereas the 30- to 60-Hz intracortical oscillation was sustained.

#### The temporal binding theory

One of the more prominent challenges of cognition is the integration of features into gestalt entities. How does the brain know that the features belong to the same object? Conceptual problems arise when binding is considered as strictly intracortical (i.e., Eckhorn et al. 1988; Gray et al. 1989). Intracortical binding through oscillation essentially solves the problem using circular logic. The cortex binds object features to identify the object, but to bind the features the cortex needs to know in advance that they are part of the same object. This loop requires a homunculus to extract the advanced knowledge. From a mathematical perspective, communication channels cannot create information; information can only be preserved or lost (Shannon 1948). Therefore if we consider synchrony to be informative to the perceptual process, some representation of that information must also be available in the retina.

Given these constraints, we would suggest that cortical synchrony starts with the visual stimulus and the retinal input.

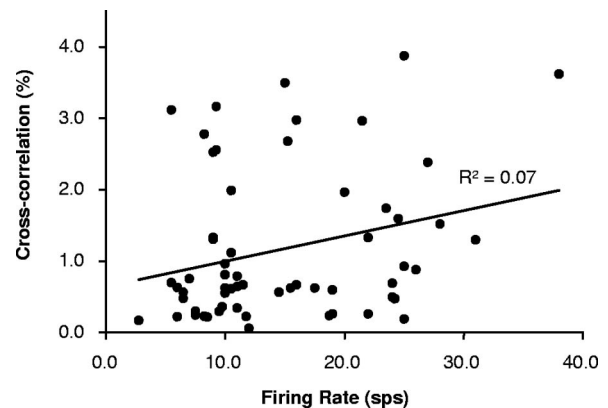


FIG. 13. Scatter plot and regression analysis ( $n = 60$  pairs of cells) for the relationship between cross-correlogram peaks and the average firing rate.

Spatial and temporal correlations in the visual scene cause synchronous activation of populations of retinal cells. This leads to matching cortical latencies, triggering synchronization. Transient synchrony occurs with either dynamic or novel stimuli (Kruse and Eckhorn 1996) propagating from retina to LGN to cortex (Castelo-Branco et al. 1998; Neuenschwander et al. 2002). Kruse and Eckhorn (1996) proposed that transient synchrony and oscillatory synchronization were distinct, but we suggest instead that sustained steady-state stimulation creates oscillation that maintains the transient form of synchrony.

Oscillation occurs more often for drifting versus stationary gratings (Engel et al. 1990) and might therefore be a mechanism that is relevant only for motion processing. However, with stimulus flicker or alert monkeys (allowing residual eye movements), stationary gratings also induce gamma oscillation (Eckhorn et al. 1988; Friedman-Hill et al. 2000). When testing both stationary and drifting gratings, cells can oscillate for both forms of stimulation, only stationary stimuli, or only drifting stimuli (Friedman-Hill et al. 2000). These different populations might form subclasses that serve different types of analyses and project to different locations. If oscillation and synchrony constituted a mechanism to propagate information reliably, one might expect cells that oscillate only for stationary stimuli to project to object-recognition regions (e.g., V4, IT, etc.) and cells that oscillate only for drifting stimuli to project to motion-processing areas (e.g., V2, MT, etc.).

The successive layers of the pathway from retina through extrastriate cortex could, as nonlinear networks, progressively extract higher-order spatial and temporal properties of visual stimuli. At the level of the striate cortex, the correlations become progressively harder to detect as stimulus properties (e.g., Purpura et al. 1994) become more abstract and global. This might explain why it is typically more difficult to find both synchronization and the appropriate form of stimulation to identify the representation of visual information at higher levels of the visual system (Usrey and Reid 1999).

Therefore we prefer to think of synchrony as a mechanism for reliable signal transmission that extracts higher-order correlations as a *gestalt* rather than as an active binding mechanism that represents a secondary code to link a system of simple feature extraction. Eckhorn et al. (1988) proposed the hypothesis that global feature extraction (i.e., detection of complex structures) was simply a higher-order form of feature extraction that arises in cortex. We believe that “global properties” (extending beyond the boundaries of single receptive fields) might simply be embodied in the higher-order stimulus correlations revealed in the synchronous firing in the cortex. Higher-order feature extraction could be interpreted as the binding of lower-order local features, but the importance in the distinction between an active intracortical binding mechanism versus higher-order filtering is that the latter process will not run into the circular logic contradiction described above and might not pass every possible test of feature binding (e.g., Shadlen and Movshon 1999).

In conclusion, we have described a simple and straightforward system that allows the selective synchronization of particular subgroups of cells by the cortical network. The synchronized assemblies can extract salient visual information such as coherent visual structure. The scheme is supported by our data showing a strong relationship between the overall

strength of cortical synchrony and the initial strength of the cortical synchrony (see also Fries et al. 2001). The transient nature of the synchronization supports both models (Opara and Wörgötter 1996) and psychophysical data (Hancock and Phillips 2004; Lee and Blake 1999; Usher and Donnelly 1998) that suggest a fast cortical response latency-dependent form of binding that does not rely on top-down mechanisms. Our results also suggest that gamma oscillations maintain the transient form of synchrony so that the brain can retain and use this information for higher cognitive (i.e., top-down) processing.

#### ACKNOWLEDGMENTS

We thank J. Allison and H. Brown for contributions as coauthors in the original study for the data set described in this article. We are very grateful to the anonymous reviewers for many helpful and constructive comments on the manuscript.

#### GRANTS

This work was supported by National Eye Institute Grant RO1EY-03778-20 and RO1EY-014680-01.

#### REFERENCES

- Aertsen AMHJ, Gerstein GL, Habib MK, and Palm G. Dynamics of neuronal firing correlation: modulation of “effective connectivity.” *J Neurophysiol* 61: 900–917, 1989.
- Agmon A and Connors BW. Repetitive burst-firing neurons in the deep layers of mouse somatosensory cortex. *Neurosci Lett* 99: 137–141, 1989.
- Bair W, Koch C, Newsome W, and Britten K. Power spectrum analysis of bursting cells in area MT in the behaving monkey. *J Neurosci* 14: 2870–2892, 1994.
- Bringuier V, Frengac Y, Baranyi A, Debanne D, and Schulz DE. Synaptic origin and stimulus dependency of neuronal oscillatory activity in the primary visual cortex of the cat. *J Physiol* 500: 751–774, 1997.
- Brumberg JC, Nowak LG, and McCormick DA. Ionic mechanisms underlying repetitive high-frequency burst firing in supragranular cortical neurons. *J Neurosci* 20: 4829–4843, 2000.
- Castelo-Branco M, Neuenschwander S, and Singer W. Synchronization of visual responses between the cortex, lateral geniculate nucleus, and retina in the anesthetized cat. *J Neurosci* 18: 6395–6410, 1998.
- Cattaneo A, Maffei L, and Morrone C. Two firing patterns in the discharge of complex cells encoding different attributes of the visual stimulus. *Exp Brain Res* 43: 115–118, 1981a.
- Cattaneo A, Maffei L, and Morrone C. Patterns in the discharge of simple and complex visual cortical cells. *Proc R Soc Lond B Biol Sci* 212: 279–297, 1981b.
- Connors BW and Gutnick MJ. Intrinsic firing patterns of diverse neocortical neurons. *Trends Neurosci* 13: 99–104, 1990.
- Cunningham MO, Davies CH, Buhl EH, Kopell N, and Whittington MA. Gamma oscillations induced by kainite receptor activation in the entorhinal cortex in vitro. *J Neurosci* 23: 9761–9769, 2003.
- DeBusk BC, DeBruyn EJ, Snider RK, Kabara JF, and Bonds AB. Stimulus-dependent modulation of spike burst length in cat striate cortical cells. *J Neurophysiol* 78: 199–213, 1997.
- de Oliveira SC, Thiele A, and Hoffmann KP. Synchronization of neuronal activity during stimulus expectation in a direction discrimination task. *J Neurosci* 17: 9248–9260, 1997.
- Dobrunz LE and Stevens CF. Response of hippocampal synapses to natural stimulation patterns. *Neuron* 22: 157–166, 1999.
- Eckhorn R, Bauer R, Jordan W, Brosch M, Kruse W, Munk M, and Reitboeck HJ. Coherent oscillations: a mechanism of feature linking in the visual cortex? *Biol Cybern* 60: 121–130, 1988.
- Engel AK, König P, Gray CM, and Singer W. Stimulus-dependent neuronal oscillations in cat visual cortex: inter-columnar interactions as determined by cross-correlation analysis. *Eur J Neurosci* 2: 588–606, 1990.
- Ernst U, Pawelzik K, and Geisel T. Synchronization induced by temporal delays in pulse-coupled oscillators. *Phys Rev Lett* 74: 1570–1573, 1995.
- Ernst U, Pawelzik K, and Geisel T. Delay-induced multistable synchronization of biological oscillators. *Phys Rev E Stat Phys Plasmas Fluids Relat Interdiscip Top* 57: 2150–2162, 1998.

- Frenceschetti S, Guatto E, Panzica F, Sancini G, Wanke E, and Avanzini G.** Ionic mechanisms underlying burst firing in pyramidal neurons: intracellular study in rat sensorimotor cortex. *Brain Res* 696: 127–139, 1995.
- Friedman-Hill S, Maldonado PE, and Gray CM.** Dynamics of striate cortical activity in the alert macaque: I. Incidence and stimulus-dependence of gamma-band neuronal oscillations. *Cereb Cortex* 10: 1105–1116, 2000.
- Frien A and Eckhorn R.** Functional coupling shows stronger stimulus dependency for fast oscillations than for low-frequency components in striate cortex of awake monkey. *Eur J Neurosci* 12: 1466–1478, 2000.
- Frien A, Eckhorn R, Bauer R, Woelbern T, and Gabriel A.** Fast oscillations display sharper orientation tuning than slower components of the same recordings in striate cortex of the awake monkey. *Eur J Neurosci* 12: 1453–1465, 2000.
- Fries P, Neuenschwander S, Engel AK, Goebel R, and Singer W.** Rapid feature selective neuronal synchronization through correlated latency shifting. *Nat Neurosci* 4: 194–200, 2001.
- Galarreta M and Hestrin S.** Spike transmission and synchrony detection in networks of GABAergic interneurons. *Science* 292: 2295–2299, 2001.
- Ghose GM and Freeman RD.** Oscillatory discharge in the visual system: does it have a functional role? *J Neurophysiol* 68: 1558–1574, 1992.
- Ghose GM and Freeman RD.** Intracortical connections are not required for oscillatory activity in the visual cortex. *Vis Neurosci* 14: 963–979, 1997.
- Gray CM, Engel AK, König P, and Singer W.** Synchronization of oscillatory neuronal responses in cat striate cortex: temporal properties. *Vis Neurosci* 8: 337–347, 1992.
- Gray CM, König P, Engel AK, and Singer W.** Oscillatory responses in cat visual cortex exhibit inter-columnar synchronization which reflects global stimulus properties. *Nature* 338: 334–337, 1989.
- Gray CM and McCormick DA.** Chattering cells: superficial pyramidal neurons contributing to the generation of synchronous oscillations in the visual cortex. *Science* 274: 109–113, 1996.
- Grossberg S.** Adaptive pattern classification and universal recoding: II. Feedback, expectation, olfaction, illusions. *Biol Cybern* 23: 187–202, 1976.
- Grossberg S.** How does a brain build a cognitive code? *Psych Rev* 87: 1–51, 1980.
- Hancock P and Phillips WA.** Pop-out from abrupt visual onsets. *Vision Res* 44: 2285–2299, 2004.
- Harris KD, Henze DA, Csicsvari J, Hirase H, and Buzsáki G.** Accuracy of tetrode spike separation as determined by simultaneous intracellular and extracellular measurements. *J Neurophysiol* 84: 401–414, 2000.
- Harris KD, Hirase H, Leinekugel X, Henze DA, and Buzsáki G.** Temporal interaction between single spikes and complex cell bursts in hippocampal pyramidal cells. *Neuron* 32: 141–149, 2001.
- Hayek FA.** *The Sensory Order*. Chicago, IL: University of Chicago Press, 1952.
- Hebb DO.** *The Organization of Behavior: A Neuropsychological Theory*. New York: Wiley, 1949.
- Jagadeesh B, Gray CM, and Ferster D.** Visually evoked oscillations of membrane potential in cells of cat visual cortex. *Science* 257: 552–554, 1992.
- König P.** A method for the quantification of synchrony and oscillatory properties of neuronal activity. *J Neurosci Methods* 54: 31–37, 1994.
- Kruse W and Eckhorn R.** Inhibition of sustained gamma oscillations (35–80 Hz) by fast transient responses in cat visual cortex. *Proc Natl Acad Sci USA* 93: 6112–6117, 1996.
- Lebedev MA and Wise SP.** Oscillations in the premotor cortex: single-unit activity from awake, behaving monkeys. *Exp Brain Res* 130: 195–215, 2000.
- Lee SH and Blake R.** Detection of temporal structure depends on spatial structure. *Vision Res* 39: 3033–3048, 1999.
- Lisman JE.** Bursts as a unit of neural information: making unreliable synapses reliable. *Trends Neurosci* 20: 38–43, 1997.
- Mandl G.** Coding for stimulus velocity by temporal patterning of spike discharges in visual cells of cat superior colliculus. *Vision Res* 33: 1451–1475, 1993.
- Milner P.** A model for visual shape recognition. *Psychol Rev* 81: 521–535, 1974.
- Molotchnikoff S, Shumikhina S, and Moison L-E.** Stimulus-dependent oscillations in the cat visual cortex: differences between bar and grating stimuli. *Brain Res* 731: 91–100, 1996.
- Mountcastle VB, Steinmetz MA, and Romo R.** Frequency discrimination in the sense of the flutter: psychological measurements correlated with post-central events in behaving monkeys. *J Neurosci* 10: 3032–3044, 1990.
- Mountcastle VB, Talbot WH, Sakata H, and Hyvarinen J.** Cortical neuronal mechanisms in flutter-vibration studies in unanesthetized monkeys: neuronal periodicity and frequency discrimination. *J Neurophysiol* 32: 452–484, 1969.
- Nase G, Singer W, Monyer H, and Engel AK.** Features of neuronal synchrony in mouse visual cortex. *J Neurophysiol* 90: 1115–1123, 2003.
- Neuenschwander S, Castelo-Branco M, Baron J, and Singer W.** Feed-forward synchronization: propagation of temporal patterns along the retinohalamocortical pathway. *Philos Trans R Soc Lond B Biol Sci* 357: 1869–1876, 2002.
- Nordhausen CT, Maynard EM, and Normann RA.** Single unit recording capabilities of a 100 microelectrode array. *Brain Res* 726: 129–140, 1996.
- Nowak LG, Azouz R, Sanchez-Vives MV, Gray CM, and McCormick DA.** Electrophysiological classes of cat primary visual cortical neurons in vivo as revealed by quantitative analyses. *J Neurophysiol* 89: 1541–1566, 2003.
- Nowak LG, Munk MHJ, James AC, Girard P, and Bullier J.** Cross-correlation study of the temporal interactions between areas V1 and V2 of the macaque monkey. *J Neurophysiol* 81: 1057–1074, 1999.
- Opara R and Wörgötter F.** Using visual latencies to improve image segmentation. *Neural Comp* 8: 1493–1520, 1996.
- Purpura KP, Victor JD, and Katz E.** Striate cortex extracts higher-order spatial correlations from visual textures. *Proc Natl Acad Sci USA* 91: 8482–8486, 1994.
- Rietboeck HJ, Eckhorn R, and Pabst M.** A model of figure/ground separation based on correlated neural activity in the visual system. In: *Synergetics of the Brain*, edited by Haken H. New York: Springer-Verlag, 1987.
- Samonds JM, Allison JD, Brown HA, and Bonds AB.** Cooperation between area 17 neuron pairs enhances fine discrimination of orientation. *J Neurosci* 23: 2416–2425, 2003.
- Samonds JM, Allison JD, Brown HA, and Bonds AB.** Cooperative synchronized assemblies enhance orientation discrimination. *Proc Natl Acad Sci USA* 101: 6722–6727, 2004.
- Samonds JM and Bonds AB.** From another angle: differences in cortical coding between fine and coarse discrimination of orientation. *J Neurophysiol* 91: 1193–1202, 2004.
- Shadlen MN and Movshon JA.** Synchrony unbound: a critical evaluation of the temporal binding hypothesis. *Neuron* 24: 67–77, 1999.
- Shannon CE.** A mathematical theory of communication. *Bell Syst Tech J* 27: 379–423, 623–656, 1948.
- Silva-Barrat C, Aranedo S, Menini C, Champagnat J, and Naquet R.** Burst generation in neocortical neurons after GABA withdrawal in the rat. *J Neurophysiol* 67: 715–727, 1992.
- Snider RK.** *The Role of Cortical Burst Firing in the Modulation of Functional Connectivity in Cat Striate Cortex* (PhD thesis). Nashville, TN: Vanderbilt University, 1997.
- Snider RK and Bonds AB.** Classification of non-stationary neural signals. *J Neurosci Methods* 84: 155–166, 1998.
- Snider RK, Kabara JF, Roig BR, and Bonds AB.** Burst firing and modulation of functional connectivity in cat striate cortex. *J Neurophysiol* 80: 730–744, 1998.
- Tovee MJ and Rolls ET.** Oscillatory activity is not evident in the primate temporal visual cortex with static stimuli. *Neuroreport* 3: 369–372, 1992.
- Traub RD, Cunningham MO, Gloveli T, LeBeau FEN, Bibbig A, Buhl EH, and Whittington MA.** GABA-enhanced collective behavior in neuronal axons underlies persistent gamma-frequency oscillations. *Proc Natl Acad Sci USA* 100: 11047–11052, 2003.
- Traub RD, Jeffreys JGR, and Whittington MA.** *Fast Oscillations in Cortical Circuits*. Cambridge, MA: MIT Press, 1999, p. 185–236.
- Traub RD and Miles R.** *Neuronal Networks of the Hippocampus*. New York: Cambridge Univ. Press, 1991, p. 37–43.
- Ts'o DY, Gilbert CD, and Wiesel TN.** Relationships between horizontal interactions and functional architecture in cat striate cortex as revealed by cross-correlation analysis. *J Neurosci* 6: 1160–1170, 1986.
- Tsodyks M, Mitkov I, and Somplinsky H.** Pattern of synchrony in inhomogeneous networks of oscillators with pulse interactions. *Phys Rev Lett* 71: 1280–1283, 1993.
- Tsodyks MV and Markham H.** The neural code between neocortical pyramidal neurons depends on neurotransmitter release probability. *Proc Natl Acad Sci USA* 94: 719–723, 1997.
- Usher M and Donnelly N.** Visual synchrony affects binding and segmentation in perception. *Science* 394: 179–182, 1998.

- Usrey WM and Reid RC.** Synchronous activity in the visual system. *Annu Rev Neurosci* 61: 435–456, 1999.
- Usrey WM, Reppas JB, and Reid RC.** Paired-spike interactions and synaptic efficacy of retinal inputs to the thalamus. *Nature* 395: 384–387, 1998.
- Varela JA, Sen K, Gibson J, Fost J, Abbott LF, and Nelson SB.** A quantitative description of short-term plasticity at excitatory synapses in layer 2/3 of rat primary visual cortex. *J Neurosci* 17: 7926–7940, 1997.
- von der Malsburg C.** *The Correlation Theory of Brain Function*. Internal Report. Goettingen, Germany: Max-Planck Institute for Biophysical Chemistry, 1981.
- von der Malsburg C and Schneider W.** A neural cocktail-party processor. *Biol Cybern* 54: 29–40, 1986.
- Young MP, Tanaka K, and Yamane S.** On oscillating neuronal responses in the visual cortex of the monkey. *J Neurophysiol* 67: 1464–1474, 1992.